Applied Energy 263 (2020) 114620

Contents lists available at ScienceDirect

Applied Energy

journal homepage: www.elsevier.com/locate/apenergy

On the water footprint in power production: Sustainable design of wet cooling towers

Lidia S. Guerras, Mariano Martín*

Department of Chemical Engineering, University of Salamanca, Plz. Caídos 1-5, 37008 Salamanca, Spain

HIGHLIGHTS

- Water footprint determines the sustainability of the future power system.
- We address the sustainable design of NDWCT, the more efficient cooling systems.
- Rigorous and simple models are developed for column design and water consumption estimation.
- The effect of the power plant location on the water footprint and on the cost is presented.
- Hotter climates with high humidity increase the water consumption and system cost.

ARTICLE INFO

Keywords:
Cooling towers
Natural draft
Water consumption
Water – energy nexus
Cost estimation

ABSTRACT

Renewable based power plants must be installed where the main resource is available. The weather affects the design and the water footprint of these plants. Two types of power cycles, a regenerative Rankine cycle, representing biomass and solar thermal plants, and the combined cycle, corresponding to biogas or gasification based processes, are studied. The facilities are modeled unit by unit in detail to compute the cycle yield, the condenser duty, the water consumption and the natural draft wet cooling tower geometry for its sustainable design. Hot regions, appropriate for solar facilities, and humid regions require larger and more expensive towers. Areas with high solar availability also show larger consumption of water presenting a tradeoff for a future renewable based power system. In addition, design guidelines and surrogate models to estimate water consumption, cooling tower size and its cost as a function of the climate have also been developed. The surrogates are useful for the analysis on the water footprint of a renewable based power system that substitutes the fossil based one.

1. Introduction

The Water-Energy (WE) nexus has become an important criterion for the analysis of the sustainable growth of society [1]. This nexus is of paramount importance in the power industry due to the strong link between water consumption and electricity production [2,3]. Most power plants use wet cooling towers as the technology of choice because of their efficiency [4,5], but their operation relies on the availability of water. These units cool down the water used in condensing the exhaust steam from the turbine at the expense of evaporating a fraction of it. Cooling towers play a key role in the cleaner production of power to avoid thermal load released to rivers [2,6], but the make-up water represents the consumption of water in the production of electricity. On average, Rankine based power plants consume around 2 L/kWh in their operation on average [6–10], while combined cycles are more efficient, presenting consumptions of around 1 L/kWh [11]. The current trend towards a more sustainable energy system results in the penetration of resources such as biomass, solar and wind into the energy mix [12]. The main issue related to the use of renewable resources is that the location of the facilities that transform them into electricity is highly dependent on the availability of the resources. In most cases the weather conditions are not the most appropriate for the operation of cooling technologies and, in particular, cooling towers. In a future where water scarcity is also a major concern [13], the analysis of the water footprint of the emerging power system is an important index for its sustainability [14].

Different dry cooling systems are being studied recently aiming at dealing with the water consumption on power plants, and in particular in concentrated solar power plants (CSP). Among these designs it is important to highlight the A-frames, air cooler condensers with a

* Corresponding author.
E-mail address: mariano.m3@usal.es (M. Martín).

https://doi.org/10.1016/j.apenergy.2020.114620
Received 4 November 2019; Received in revised form 3 February 2020; Accepted 5 February 2020
Available online 26 February 2020

Nomenclature

A	cross sectional area (m^2)
A_{HX}	area of the heat exchanger (m^2)
b	characteristic dimension (m)
c_h	humid air heat capacity ($kcal/kg_{dry\ air}$)
Cp	Heat capacity (kcal/kg °C)
d	design variables
d_H	top diameter of the tower (m)
D_{base}	base diameter of the tower (m)
f_{air}	flow of air (kg/s)
f_{Wa}	flow of water (kg/s)
F_B	blowdown flow (kg/s)
F_D	drift flow (kg/s)
F_E	evaporation flow (kg/s)
F_M	make-up flow (kg/s)
g	gravity (m/s^2)
G_{flux}	flow of air per unit area (kg/m^2s)
h_L	resistance to heat transfer ($kcal/m^2{\cdot}s$)
h_c	air entrance height, (m)
h_{liquid}	liquid enthalpy (kcal/kg)
h_{steam}	steam enthalpy (kcal/kg)
H	humid air enthalpy (kcal/kg)
k_y	resistance to mass transfer ($kg\ /m^2s$)
L_{flux}	flow of water per unit area (kg/m^2s)
L/V	ratio between the water and the air flow rates across the column in mass
M_i	molar weight of species i (kg/kmol)
N_i	number of velocity heads of pressure drop due to item i.
p	pressure (bar)
P_{Height}	height of the packed section (m)
Power	mean power (MW)
$Q_{(unit)}$	thermal energy at unit (kW)
R	gas constant (atm·L/mol·K)
r_t	minimum radius of the hyperboloid (m)
S	specific contact area (m^{-1})
t	air temperature (°C)
T	water temperature across the cooling tower (°C)
$T_{(unit)}$	stream temperature (°C)
T_{Height}	height of the cooling tower (m)
ν	air velocity (m/s)
V_{shell}	volume of shell (m^3).
$W_{(unit)}$	electrical energy unit (kW)
$Y_,$	air moisture (kg moisture per kg dry air)
Z_H	height of the section of the tower (m)
Z_u	height of the section of the tower (m)
ΔH_f	formation energy (kW)
ΔP_{Loss}	pressure drop (Pa)
$\Delta P_{Generated}$	driving force for the pressure (Pa)

Subindex

i	interphase conditions
in	inlet
L	liquid bulk
g	gas bulk
out	outlet
sat	saturation condition
Wa	component water

Symbols

ρ	air density (kg/m^3)
η_c	efficiency of the compressor

Units

CT	cooling tower
HX	heat exchanger
Turb	turbine
Spl	splitter
Furnace	
Boiler	

bundle of pipes in the form of an A [15]. While these systems are interesting for solar applications, they use up to 10% of the power from the facility to condense the exhaust [5]. Alternatively, natural draft dry cooling towers (NDDCT) can also be used. They are similar to wet cooling towers but within the structure a heat exchanger is built [16]. Its operation relies on convective heat transfer [17]. Although, NDDCT operation does not consume water, it is highly dependent on the weather conditions [18] and particularly on the crossflow wind [19]. It has been proved that for hot days pre wet cooling is recommended [20]. Thus, the high efficiency of wet cooling towers, the fact that the power industry is used to operate them [4] and the recent findings that show that even under scarce water availability wet cooling towers are competitive and offer a sustainable performance versus dry cooling [5] encourages improving the sustainability and efficiency of these units towards their implementation within renewable based power facilities.

The design of natural draft wet cooling towers (NDWCT) is an area that combines the structural design of the unit and the unit operation of water cooling. As a result, two lines or work have been pursued, either structural analysis or the performance of the tower. On the one hand, studies have focused on the structural design of the tower [21] presenting new designs [22], the evolution of cooling tower sizing over time [23] as well as the estimation of the cost of the unit from the mechanical and structural points of view [24,25]. On the other hand, the evaluation of the gas-liquid contact responsible for water cooling has been studied experimentally [26] and theoretically [27] evaluating the performance [28], optimizing it [29], presenting design rules [30] as well as current efforts to evaluate their operation within concentrated solar power (CSP) plants [31], performing sensitivity analysis on the operation [32] as well as economic [33] and environmental analysis [34] of the tower, to optimize their performance when used for CSP plants [35]. Simulation [36] and mathematical optimization [37] approaches have been used to improve the performance of the tower analyzing the transport phenomena involved in the operation, including the systematic comparison of various fillings [38,39]. However, to the best of our knowledge, design of NDWCT considering structural and gas-liquid contact simultaneously has not been addressed. In addition, to achieve the goal of sustainable power production the use of renewable resources to produce electricity is not enough. The sustainable design of the cooling technologies is also to be addressed. A sustainable design must take into account the simultaneous analysis of the structure, responsible for use of material, and the unit cost, and the gas-liquid contact, linked to the performance and the consumption of water. However, typically the estimation of the cost of cooling towers is based on the heat load rejected alone [40,41], while the size of the tower is a function of the weather [42]. For instance, the tower size for the same cooling load is almost twice in the northwestern of Spain compared to the south east [35]. Therefore, the cost estimation methods available in the literature [40,41] do not capture the effect of the location of the unit that is paramount for the design of the future power system towards reducing its environmental impact, including the water footprint. In addition, the analysis of water consumption has received less attention. Over the years research has focused on evaluating the

operation of the cooling towers at different seasons [43] and climatic zones [44], including the effect of climate change on the future design of the towers [45], monitoring their efficiency over time [46] and defining a methodology to evaluate that performance [47], presenting profiles of data on the water withdrawal and consumption [48], reporting average values for the consumption [49] and evaluating the crosswind effect on the temperature profile experimentally [50] and on their operation [51]. The systematic evaluation of the operation of cooling towers resulted in rules of thumb [52], surrogate models [53] and the development of simplified models to estimate the evaporative loses [54–56]. Only lately, due to the concerns on future water availability have led to computing the consumption of water related to the operation of the cooling tower [3,42], comparing its performance with air cooling as a water saving alternative [57]. However, the effect of the location of the unit on the water footprint due to the weather conditions has not been evaluated nor an easy method to compute is available.

In this work an integrated mathematical formulation is developed to provide design guidelines for the design of sustainable natural draft wet cooling towers and to estimate their water footprint as a function of the power plant location. The study provides process data on the water footprint when substituting the power produced by current facilities by renewable-based resources so as to be able to select the cooling system based on performance and cost comparing dry and wet cooling alternatives. These results are needed to evaluate the future energy system where a range of resources will contribute to meet the power demand and whose availabilities are highly location dependent. To achieve that, the entire power facility is considered in the analysis. Two thermodynamic cycles are evaluated to cover all possible sources of energy in thermal plants, the Rankine and combined cycles. The facilities are modeled in detail from a process perspective to compute the power production, the cooling needs, the water consumption and the tower structure. Due to the effect of weather conditions on the design and water consumption of the tower, real data of an entire country are used. Spain is considered as a case study because it is in a vulnerable situation regarding water availability, presenting regions with moderate availability together with others where desertification is becoming an issue [57]. The model is used for a variety of climate regions such as arid ones in the South West, continental, Mediterranean, Cantabrican and Atlantic climates and validated against industrial data. This study also allows developing surrogate models for the quick prediction of the water consumption and the estimation of the cooling tower sizing and cost as a function of the location. The rest of the paper is organized as follows. In Section 2 the methodology for the sustainable design of cooling towers and the location effect on their water footprint is presented and the development of surrogates for conceptual design. Section 3 shows the details of the modelling of the entire facility, from the power island to the cooling section, including mass and energy balances, thermodynamics, rules of thumb and geometric constraints. In Section 4 the main results are discussed. Finally, Section 5 draws some conclusions.

2. Methodology

NDWCTs are widely used as cooling technology for thermal plants due to their efficiency [5]. However, their design must address the structure and water use simultaneously to improve the environmental footprint of the future energy systems, whose location is linked to the availability of the resources. This work aims at designing sustainable cooling towers and also, once installed, evaluating their water footprint across weather conditions. The analysis presented in this work, as described in Section 2.1 of the methodology, evaluates the water footprint and the cooling tower design associated to the two main thermal cycles implemented in power plants, regenerative Rankine and combined cycle. The analysis of each of the cycles is based on a detailed first principle model of the entire power plant. This model will be developed and validated versus industrial data to represent the cooling tower, including structural and gas-liquid contact features, as well as the thermodynamic cycles. The model itself will be described in Section 3. Aiming at the optimal sustainable design of the unit and consumption of water, a mathematical optimization framework is formulated. An

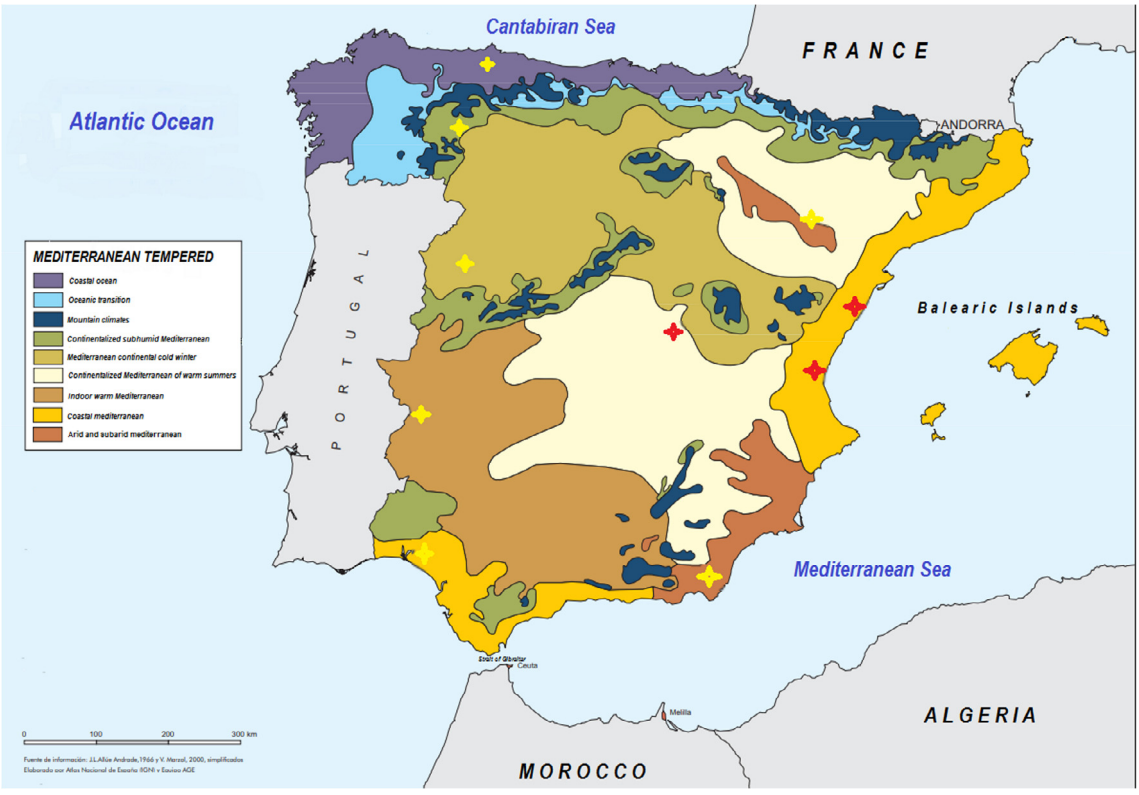

Fig. 1. Climatic regions and locations evaluated. Adapted with permission from [59]

objective function that considers sustainable parameters of the cooling tower is developed, as presented in Section 2.2, including the models described in Section 3 as constraints. The design of the cooling tower is a different problem compared to the evaluation of the water consumption. The first problem aims at the sustainable design of the cooling tower as a function of the location, and it is discussed in Section 2.3. The second one, presented in Section 2.4, addresses the effect of the weather conditions on the water consumption. Finally, for easy use of the results of this work, Section 2.5 presents the approach used to develop surrogate models to easily estimate the tower size, its cost and water consumption as a function of the facility location.

Two main results are expected from this work, the geometric design of the tower and the water consumption when a particular facility is located at a region. To present the variability in the water consumption and tower design under different weather conditions, the model is evaluated in different climate regions across Spain. The regions are selected so that all the climates are represented in the study. Fig. 1 shows the map of the climatic regions of Spain. To be representative of cold and warm regions, 10 different provinces within the main climatic areas are considered, from arid in the southeast, to oceanic in the northwest including Mediterranean hot, to Mediterranean mild in the cost, from the continental, to the steppe, covering the places where current fossil based plants are located. Furthermore, the location of current nuclear, coal and natural gas facilities, as provided by the Spanish national electric network, is considered for the selection of the locations evaluated [58]. The selected locations are represented by stars in Fig. 2.

2.1. Models structure of the thermodynamic cycles

This study considers two different cycles to represent most of the thermal power facilities no matter the energy source. The regenerative Rankine Cycle, from now on P1, consists of the mass, energy balances and thermodynamic properties described in Sections 3.1 and 3.3, see supplementary material for the full set of equations. This cycle represents the operation of a conventional coal, any fossil fuel as well as concentrated solar (CSP's) and biomass power plants. This model is written in GAMS® with around 220 equations and similar number of variables. For the combined cycle, P2, the model includes the gas treatment and the gas turbine while the Rankine cycle is modified so that the energy source is the hot flue gas from the gas turbine, as presented in Sections 3.2 and 3.3. A combined cycle can be used with natural gas, shale gas, syngas or biogas. Furthermore, it can easily be extended to biomass or coal by integrating a gasifier into the process. The model is larger, around 778 eqs. and 971 var., and it is also written in GAMS®.

2.2. Objective function

For the sustainable design of cooling towers, a number of criteria must be considered including costs and environmental impact. The Renewable Process Synthesis Index Metric (REPSIM) [60] is used to develop an objective function so as to simultaneously account for the emissions saved when substituting current coal based facilities, the emissions due to water consumption, both translated into cost using the carbon tax and the investment cost of the materials such as the shell of the cooling tower and the heat exchanger of the cooling system. Thus, the objective function becomes Eq. (1).

$$\begin{aligned} \text{Cost} = {} & C_{TAX}\left(-W_{total}\cdot CO_{2_{Power}}\cdot\tau + \ Water_C\cdot CO_{2_{Water}}\tau\right) + \frac{1}{3} \\ & \left(C_{Shell}\cdot Volume_{Shell} + C_{Wood}Volume_{Filling} + C_{HX}\right) \end{aligned} \tag{1}$$

The emissions due to the cooling tower shell and its packing can also be computed. However, since the emissions due to the material are also related to the volume of concrete, as well as its cost, it is decided not to consider both to avoid double counting of the volume of the material in the objective function. The emissions and costs due to the different items are taken from the literature as well as the carbon tax, see Table 1

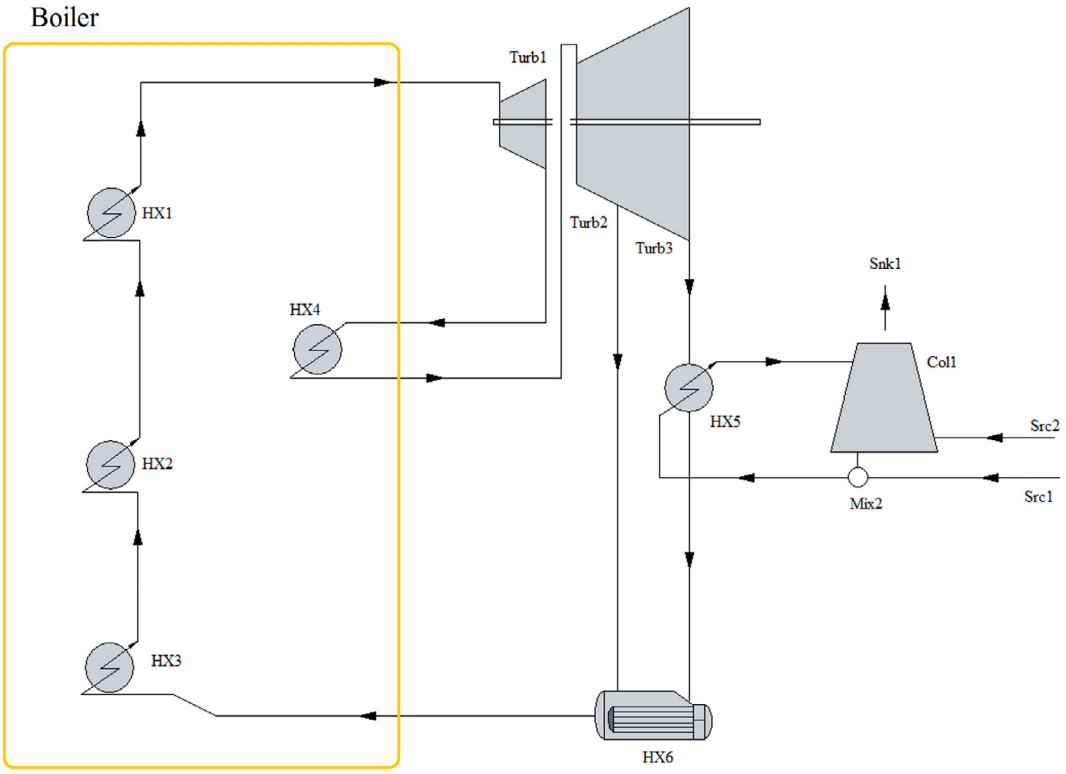

Fig. 2. Flowsheet of the facility based on a regenerative Rankine cycle.

Table 1
Parameters of the emissions and cost objective function [25,61,62]

	CO_2 Emissions	Cost	
Power	0.632 kg/kWh	50 €/t Carbon Tax	
Water Consumption	0.3 kg/m^3	50 €/t Carbon tax	
Concrete Shell	0.41 kg/L	200 €/m^3	[20,52]
Tower filling	1.33 kg/L	25 €/m^3	[20,53]

2.3. Cooling tower design problem.

The design of a unit consists of defining the features so that it is flexible to operate over time. Therefore, the sustainable design of the cooling tower is performed optimizing P1 and P2 using Eq. (1) as objective function following a worst case scenario approach over the time horizon of a year. The worst case corresponds to the month with the most complex conditions for the tower to operate, typically the one with the lowest temperatures and largest humidity, resulting in the need for a larger tower size. The tower height and the materials cost are evaluated as a function of the plant production capacity, the pressure, temperature and humidity. The problems are solved using a multi-start optimization procedure with CONOPT as the preferred solver. The model is validated versus industrial data. To evaluate the effect of the production capacity on the tower size and cost, different power plant sizes for the 10 locations are considered. For the regenerative Rankine cycle 6 plant capacities are used from 40 to 450 MW. For the combined cycle, a more efficient cycle, 5 plant sizes from 100 to 450 MW are used.

2.4. Water consumption evaluation

The water consumption of the optimal cooling tower installed under different weather conditions is evaluated by solving P1 and P2 using Eq. (1) as objective function. The problems are solved using a multi-start optimization procedure with CONOPT as preferred solver. In this case, for both cycles, the power production capacity is fixed to 350 MW, the typical size of a thermal group in coal based power plants in Spain [63]. The model is also validated versus industrial facilities data. Next, the actual weather data of the 10 locations over the entire year on a monthly basis generate a data set of 120 points, each considered as an independent design condition. Each thermodynamic cycle is evaluated over the data set to evaluate the effect of pressure, temperature and humidity on the consumption of water. Note that alternatively, we could have used a Monte Carlo approach to generate the set of combinations of the independent variables. However, by using real data, the results are expected to be more representative and allow presenting the water consumption across Spain to see the effect of the location of the facility on the use of water.

2.5. Surrogate model development

The use of the detailed models given by P1 or P2 may not be easy for early stage analysis and conceptual design. The data obtained from the optimization of the cases described along the previous two paragraphs are used to develop surrogate models for quick estimation of the tower geometry, its cost and the water consumption as a function of the weather conditions and the power plant capacity. The fitting is carried out suggesting a non-linear multivariable model that is adjusted to the results of the detailed model minimizing the error of estimation using a reduced gradient method in GAMS®. These correlations can be implemented within the current tools [40,41] to estimate the performance and the cost of the NDWCT.

3. Process model

This section is divided into the evaluation of the power islands of two different thermodynamic cycles, regenerative Rankine, and combined cycle, and the detailed design for the cooling tower. P1 defined in the Section 2 consists of the models described in Sections 3.1 and 3.3 while P2 includes the processes depicted in Sections 3.2 and 3.3.

3.1. Rankine cycle analysis

The Rankine cycle is modeled unit by unit as presented in Fig. 2. Mass and energy balances and detailed thermodynamics are used, see supplementary material for the modelling details. Here, only the major assumptions are presented.

The source of energy can be a fuel, where a boiler is used, or a solar field. For a regenerative Rankine cycle two stages are considered, production of superheated steam and steam reheating. In case a fuel is used, both steps take place within the boiler. However, in the case of CSP plants, a series of heat exchanges are used to heat up, evaporate and overheat the steam and another heat exchanger is used for the regenerative section of the cycle. The overheated steam is fed to the turbine. This unit is modeled as consisting of high, medium and low pressure sections. The pressure range of operation for each section of the turbine is taken from the literature. In the literature the high pressure turbine typically operates from 40 to 126 bar [31,64]. Thus, a range from 90 bar to 125 bar for the steam being fed to the turbine is considered. The high pressure superheated steam is expanded into a medium pressure. A range from 11 to 35 bar is allowed based on data from the literature [31,65]. A fraction of the stream is used as an extraction to reheat up the condensed steam and the rest is expanded in the low pressure turbine. This last pressure ranges from 0.05 bar to 0.31 bar [66,67]. It is also an optimization variable within the range of 0.05 to 0.35 bar. This stream can contain a small amount of vapor, up to 8%. Each turbine, low, medium and high pressure, is modeled similarly considering a non-ideal isentropic expansion. The expansion of the steam in the different turbines is assumed to have an isentropic efficiency of 0.9 [68]. The enthalpies and entropies are computed using surrogate models as a function of the pressure and temperature developed in previous works [42,68]. The total energy obtained in the system to be optimized is the sum of the ones generated at the three bodies of the turbine

3.2. Combined cycle analysis

From a gas fuel, the process consists of a treatment stage to remove sulphur hydride and other traces of undesirable species including ammonia, particles or CO_2. Next a gas turbine is used. The model for the gas turbine consists of four sections. The compression stages of air and fuel, a combustion chamber and a final gas expansion. Multistage compression with intercooling are used to model both assuming polytropic compressors, Eqs. (2)–(3). The polytropic coefficient, z, is taken to be 1.4 based on an offline simulation using CHEMCAD®. The efficiency of the compressor (η_c) is assumed to be 85% [69]. A maximum gas pressure of 40 bar is considered.

$$T_{out/compresor} = T_{in/compressor} + T_{in/compressor}\left(\left(\frac{P_{out/compressor}}{P_{in/compressor}}\right)^{\frac{z-1}{z}} - 1\right)\frac{1}{\eta_c} \quad (2)$$

$$W_{(Compressor)} = (F)\cdot\frac{R\cdot z\cdot(T_{in/compressor})}{((MW)\cdot(z-1))}\frac{1}{\eta_c}\left(\left(\frac{P_{out/compressor}}{P_{in/compressor}}\right)^{\frac{z-1}{z}} - 1\right) \quad (3)$$

The combustion chamber is modeled as an adiabatic furnace based on the stoichiometry of the combustion of the species with an excess of air. The excess is used to control the final temperature before expansion so that it is below 1600 °C, the typical upper bound for gas turbines. Complete combustion of all the species is assumed. The model is flexible so that not only natural gas but also biogas or syngas can be used, in case syngas is produced via biomass gasification.

$$Q_{(Furnace)} = \sum_h \Delta H_f(h)|_{T(Furnace,GasTurb)}\Big|_{(Furnace,GasTur)} - \sum_h \Delta H_f(h)|_{T(Compres2,Furnace)}\Big|_{(Compres2,Furnace)} - \sum_h \Delta H_f(h)|_{T(Compres3,Furnace)}\Big|_{(Compres3,Furnace)} \quad (4)$$

The hot gas is expanded in a turbine to obtain power. This last section of the gas turbine is modeled as a polytropic expansion, with z equal to 1.3, computed offline with CHEMCAD®, and with an efficiency of 85% [69]. The exhaust gas is used within a regenerative Rankine cycle that is modeled similarly to the one described in Section 3.2, but for the heat source that corresponds to the hot flue gas that generates the steam in HX8, HX19 and HX4 and overheats the expanded steam from the high pressure turbine in HX5. The rest is the same as for the previous case. Fig. 3 shows the flowsheet used to model the combine cycle plant.

3.3. Cooling tower design

The operation of the cooling tower depends on the gas-liquid contact provided by the packing. An analysis of the mass and energy transfer in this region is performed to evaluate its design. Further details of the model can be found in the supplementary material and in previous work [42]. The height of the packing is computed as given by Eq. (5), that is developed based on an energy balance to the packing.

$$P_{Height} = \frac{f_{air}}{k_y A\, S}\int_{h_1}^{h_2}\frac{dh}{h_i - h} \quad (5)$$

Mickley's method is used to solve the performance of the tower as described in previous work [42]. The operating line is determined by an energy balance between the air and the water flows, resulting in Eq. (6).

$$\frac{H_2 - H_1}{t_{L,2} - t_{L,1}} = \frac{f_{Wa}}{f_{air}} = \frac{L}{V} \quad (6)$$

The water flow, f_{Wa}, that is used to condense the exhaust steam from the turbine, is calculated from the energy balance to HX5, see supplementary material. The cooling water is heated up at most 8–10 °C across the heat exchanger, based on rules of thumb [70–72].

$$8 \leqslant (t_{L,in} - t_{L,out}) \leqslant 10 \quad (7)$$

where $t_{L,in}$ is the temperature of the water to be cooled and $t_{L,out}$ the final temperature of the water. The operation of the cooling tower requires a minimum flow of air, typically from 1.3 to 1.5 times the minimum given by the profile of the humid air enthalpy [66], calculated based on the inlet and outlet conditions of the air and water.

The water flow is cooled because a fraction is evaporated. Rules of thumb are used [72] to establish the lower bound of the water losses of the system, F_E, that determines the water make-up to the system and the humidity of the air exiting the cooling:

$$F_E \geqslant 1.8{\cdot}0.00085{\cdot}f_{Wa}(t_{L,in} - t_{L,out}) \quad (8)$$

The temperature of the air leaving the tower is calculated as the final temperature of the profile along the cooling tower. The Lewis relationship, Eq. (9), based on an energy balance [71], relates the operation line with the equilibrium line determining the temperature of the air.

$$\frac{H_i - H}{T_i - t_L} = -\frac{h_L}{k_y} \quad (9)$$

Even though the ideal operation suggests that the slope ($-h_L/k_y$) is –inf, it typically ranges between -3 and -10. The profile of the air temperature is computed as the ratio of the change on enthalpy and temperature as it exchanges moisture with the liquid flow Eq. (10).

$$\frac{(H_i - H)}{(T_i - T_g)} = \frac{dH}{dT_g} \quad (10)$$

The mass transfer coefficient, k_y, is computed using the correlation given by Coulson & Richardson [73] assuming that the contact area provided by the fillings is constant and equal to 250 m^2/m^3, where G_{flux} and L_{flux} are the cross sectional flows and S the specific contact area.

$$k_y = \left(\frac{2.95}{S}\right){\cdot}(G_{flux})^{0.72}{\cdot}(L_{flux})^{0.26} \quad (11)$$

The specific flows across the contact region are computed per the gas and liquid flows and the actual area

$$A = \left(\frac{\pi}{4}\right){\cdot}D_{base}^2 \quad (12)$$

$$G_{flux} = \frac{f_{air}}{A}; \quad (13)$$

$$L_{flux} = \frac{f_{Wa}}{A} \quad (14)$$

To compute the column diameter, a bound related to the height of the packing is added,

$$D_{Base} \geqslant 5{\cdot}P_{Height}; \quad (15)$$

The design of the structure of the cooling tower aims to provide enough driving force to allow the air flow across the tower. The driving

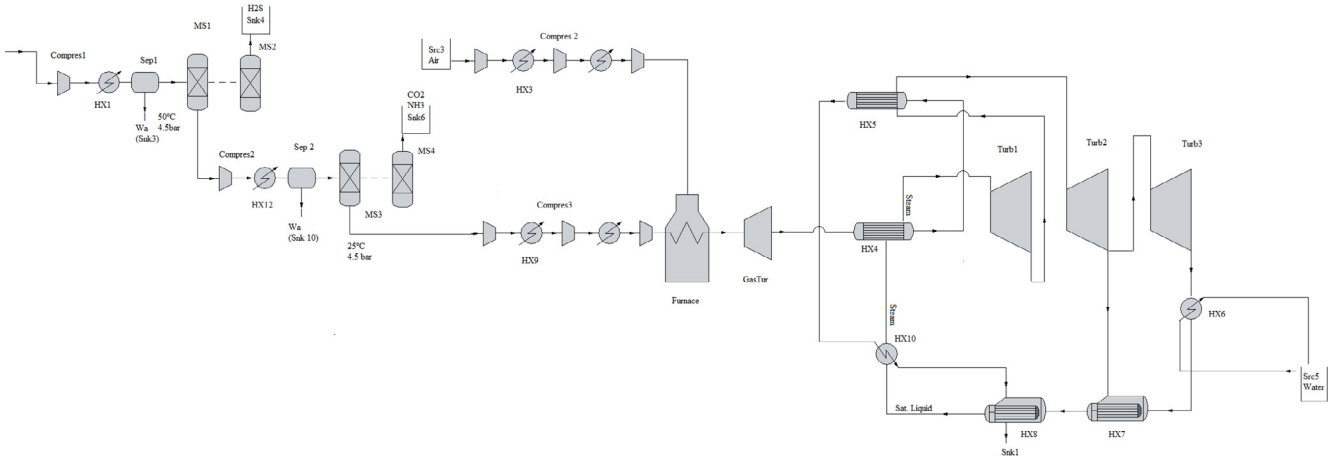

Fig. 3. Scheme of the flowsheet for a combined cycle.

force, $\Delta P_{Generated}$, is given by buoyancy, Eq. (16).

$$\Delta P_{Generated} = T_{Height} \cdot g \cdot (\rho_{g,in} - \rho_{g,out}); \quad (16)$$

where T_{height} is the total height of the tower, g is gravity and ρ_g the air density. Assuming ideal gases, the air density across the tower is computed as follows:

$$\rho_g = \left(\frac{1}{M_{air}} + \frac{Y}{M_{water}}\right)\frac{RT_g}{p} \quad (17)$$

The driving force generated by the parabolic structure must be enough to counterbalance the pressure drop generated across the support of the tower, the contraction as the air enters the structure, the packing, the pressure drop generated by the water spray generated to cooldown the water and that of the mist eliminator [24,25], see Eq. (18).

$$\Delta P_{Loss} = (N_{Mist} + N_{Support} + N_{Contraction} + N_{Spray} + N_{Packing})\rho_{air}\frac{v_{air}^2}{2}$$

where:

$$N_{Contraction} = 0.167\left(\frac{D_{base}}{h_c}\right)^2$$

$$0.02 \cdot D_{base} \leqslant h_c \leqslant 0.12 \cdot D_{base}$$

$$N_{Spray} = 0.16 \cdot h_c \cdot \left(\frac{f_{Wa,in}}{f_{air,in}}\right)^{1.32}$$

$$N_{Packing} = P_{Height} \cdot 2.36\left(\frac{Lflux}{3.391}\right)^{1.1} \cdot \left(\frac{Gflux}{3.391}\right)^{-0.64} \quad (18)$$

The driving force should be, at least, 10% larger that the pressure drop across the tower.

$$1.1 \cdot \Delta P_{Loss} \leqslant \Delta P_{Generated} \quad (19)$$

The geometry of the cooling tower is that of a hyperboloid [4], see Fig. 4. Thus, the dimensions involved in the pressure drop must comply with that geometry where each section of the hyperboloid, Z_H and Z_u, is computed using eq (20) where d_i is the diameter at Z_i, d_t is the largest diameter.

$$\frac{d_i^2}{d_t^2} - \frac{Z_i^2}{b^2} = 1 \quad \forall\, i \in \{u, H\} \quad (20)$$

The total height of the tower, T_{Height}, is given by adding the three sections in Fig. 4, where h_c is the height of the opening for the air fed to the CT.

$$T_{Height} = Z_H + Z_u + h_c \quad (21)$$

Further constraints based on rules of thumb are imposed to avoid unstable designs [25]. Almási suggested typical ratios for the dimensions of the shell as shown in Eq. (21) [74].

$$\begin{aligned} 0.55 \cdot D_{base} &\leqslant 2 \cdot r_t \leqslant 0.65 \cdot D_{base} \\ 0.61 \cdot D_{base} &\leqslant 2 \cdot r_H \leqslant 0.73 \cdot D_{base} \\ 1.25 \cdot D_{base} &\leqslant CT_{Height} \leqslant 1.5 \cdot D_{base} \\ 1.1 \cdot D_{base} &\leqslant Z_u + Z_h \leqslant 1.3 \cdot D_{base} \\ 0.92 \cdot D_{base} &\leqslant Z_u \leqslant 1.02 \cdot D_{base} \end{aligned} \quad (22)$$

Diameter ratio to prevent cold inflow around 0.58 is recommended [38]. The volume of the concrete in the tower shell can be approximated by

$$V_{Shell} = \frac{\pi}{2}(2 \cdot r_u + 2 \cdot r_H) \cdot t_s \cdot T_{Height} \quad (23)$$

where t_s is the thickness of the cooling tower shell and it is computed based on data from actual columns where t_{ratio} is 0.0023 .

$$t_s = t_{ratio} D_{Base} \quad (24)$$

The capital cost of the tower shell is approximated by Eq. (25).

$$C_s = V_{Shell} \cdot C_{conc} \quad (25)$$

where C_{conc} is the cost of concrete per unit volume, which includes the cost of construction.

The cost of the fill is given by

$$C_{fill} = V_{fi} \cdot C_{fi} = \left(\frac{\pi}{4}\right) \cdot D_{base}^2 \cdot P_{Height} \cdot C_{fi} \quad (26)$$

where C_{fi} is the cost per cubic meter of fill. See the Table 1. A detailed implementation of the CT model can be found in [35].

3.4. Water consumption

The water lost by the operation of a cooling tower is related to the recycle ratio, known as cycles of concentration (COC). Industrial practice uses COC's from 3 to 7 [75]. A value of 6 is assumed for the calculations. The water lost is due to the blow down losses, F_B, the evaporation losses, F_E and the drift. F_D. Drift is expected to be negligible in newly designed towers. F_B losses is computed as a function of the F_E as follows

$$F_B = F_E/(C.O.\ C. - 1) \quad (27)$$

Thus, the lost waster is computed by Eq. (28)

$$F_M = F_E + F_B \quad (28)$$

4. Results

The results section is divided into three major subsections. First, major operating characteristics of the power cycles are presented, Section 4.1 that will help present the different water consumption and cooling tower size for the two thermodynamic cycles. Next, in Section 4.2 the design problem is addressed, by presenting the geometric features of the cooling towers required across different climates are presented and validated versus real plant data. In addition, the effect of the weather conditions on the tower height, the characteristic variable of the cooling tower, and on the cost is evaluated and validated. Finally, surrogate models are developed for quick estimation of both. The final section of the results focuses on the water-energy nexus, Section 4.3. The effect of the weather conditions on the consumption of water is analyzed and once validated, surrogate models are developed as a function of temperature, humidity and pressure.

4.1. Operation of the renewable based thermodynamic cycles

In Section 2, the thermodynamic cycles, regenerative Rankine and combined cycle, that are used for power production in thermal plants from not only renewable resources but also fossil resources are described. Their performance determines the cooling needs. The major results of the operation of both cycles are reported in this section in the form of cooling requirements. Table 2 shows the cooling load required per kW of power produced and, in the case of the combined cycle, the contribution of each of the two turbines towards the power plant

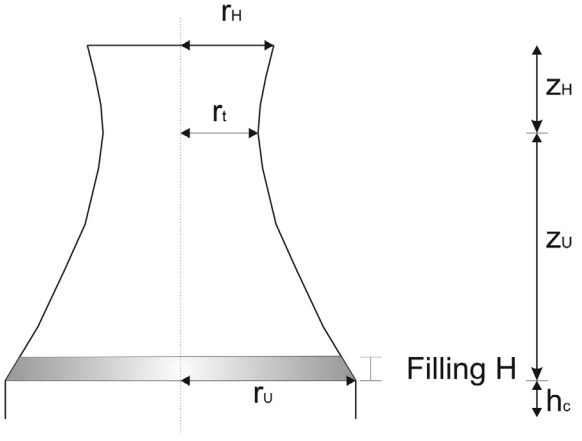

Fig. 4. Scheme of the structure of the cooling tower.

Table 2
Thermodynamic cycle cooling needs.

Definition	
Cooling rate to power (Rankine Cycle)	1.18
Cooling rate to power (Combined Cycle)	0.56
Cooling rate to power Including gas turbine cooling (Combined Cycle)	0.67
Steam turbine contribution (Combined Cycle)	0.45

operation, steam turbine production corresponds to 45% of the total power obtained in the combined cycle. It is important to note that the energy integrated within the combined cycle reduces the cooling needs almost by half. This fact will not only determine the tower size but also the consumption of water related to that particular cycle and raw material as it will be presented in the following sections.

In addition, it is fairly straight forward to use the models presented in Section 2 to compute the power-to-feed ratio. Table 3 shows the operation of the Rankine and the combined cycle from different renewable resources. The power produced per kg of raw material using the Rankine cycle is computed based on the LHV of the biomass/biowaste. Alternatively, biomass can be used within an Integrated Gasification Combined cycle (IGCC) scheme via the production of biosyngas from biomass. Using the model developed by Vidal and Martín [63], the syngas composition and flowrate per kg of biomass used can be calculated. Biosyngas composition can be fed to the model described in Section 2 for the combined cycle to compute the yield to power, see Table 3. Note that the use of biosyngas is more efficient than using directly the biomass, due to the water decomposition within the process to generate hydrogen. Instead of syngas or natural gas, biogas without upgrading can also be used as raw material for the combined cycle. The composition of the biogas before upgrading is computed from [68]. By optimizing the model presented in this paper, it is possible to compute the power obtained per kg of waste, see Table 3. These ratios represent the operation of power facilities based on renewable resources that together with the water consumption provide the basis for the capabilities of using waste and biomass in the transition of the power industry. For further information of CSP plants we refer to previous work [37,42]. .

4.2. Sustainable design of cooling towers

4.2.1. Geometric design across climates

Cooling tower sizing and costing in typically based on cooling load [41]. However, the weather conditions play an important role on the operation and also on the water-energy nexus [37]. For tower sizing, as described in Section 2.3, the worst case scenario is used at the 10 different places. Evaluating summer and winter, it turned up that January was the most challenging month in terms of the operation of the cooling tower due to the cold weather and high humidity of the air. The tower size across Spain is computed. Analyzing the results, several conclusions can be drawn. It was found that the major tower dimensions can be related to the tower height that can be used as characteristic variable of the tower size. Using it as a reference, a number of ratios between geometric variables are computed representing the main tower features. Table 4 shows the results. These ratios held in all designs. It is possible to see that the tower height is suggested to be 25% larger than the base diameter. Another interesting feature is the ratio between the base and the top diameters. Typically, the top diameter is 60% that of the base. In addition to the geometric ratios, the effect of the climate on the tower size is represented in Fig. 5. As it was expected, the tower size increases with the production capacity, since larger cooling needs are to be removed, see also Table 2. However, it is more interesting to see the effect of the site, given by the temperature, humidity and pressure, on the tower height. In general, larger towers are required towards the South-East. The lower the relative humidity and the higher the temperature, the larger the tower size. Evaluating the tower cost as a function of the site, the trends and conclusions are similar to those presented for the tower height because the tower size can be represented by its height as shown in Table 4. Note that CSP facilities are being built to the South and South-East because of the high solar incidence. The location of CSP plants shows a tradeoff between power produced and the cost in cooling facilities [37,44].

Table 4
Major rules for cooling tower design (40–450 MW)

Definition	
Tower height to Base diameter	1.25
Tower height to entrance height	10.41
Base diameter to Opening diameter	1.64
Zh to tower height	0.13
Zu to tower height	0.77

The geometric ratios presented in Table 2 are compared with two industrial towers whose geometry is reported in detail in the literature [21]. The height to diameter and the top to bottom diameter ratios are 1.38 and 1.72 for the Gundremmingen tower in Germany and 1.48 and 1.53 for the 200 m tall project. Both ratios are close to the ones reported in Table 2 of 1.25 and 1.64, validating the model results. However, a more sustainable design shows values in between the values of the two industrial towers. With regards to the heights of the difference sections of the tower, the optimization reports values of 0.13 and 0.77 respectively. For the Gundremmingen tower the values are 0.22 and 0.70, while for 200 m tall one, ratios of 0.3 and 0.64 are reported. The bottom section is always larger than the top one, but a more sustainable design suggests a taller lower section.

4.2.2. Simplified models for tower sizing and costing

The results show that the tower size depends on the weather as it was presented in Fig. 5. To provide with information at an early stage and for conceptual level design, surrogate models are developed to estimate tower size and cost as a function of the production capacity of the facility and the weather conditions. Since the tower can be characterized by its height, see Table 4, the tower sizing can be carried out by developing a surrogate model of the tower height as a function of the power plant capacity, the pressure, the temperature and the humidity. The rest of the dimensions are computed from the ratios presented in Table 4. This surrogate model can be implemented in any design tool, i.e. [40,41] for conceptual tower design and costing. Note that the Rankine and the combined cycles have several differences and show different tower sizes. Therefore, two sets of surrogate models have been developed, one set per cycle, to characterize the tower height and its

Table 3
Renewable based power plant yields.

Raw material	Rankine	Combined cycle
Biomass	6757 kJ/kg of wet biomass	Syngas comp. (CO_2 = 0.013; CO = 0.898; H_2 = 0.089) 7663 kJ/kg wet biomass
Biogas	NA	Biogas comp. (Wa = 0.12; CO_2 = 0.47; CH_4 = 0.385; N_2 = 0.02; O_2 = 0.006; NH_3 = 0.000) 3023 kJ/kg food waste

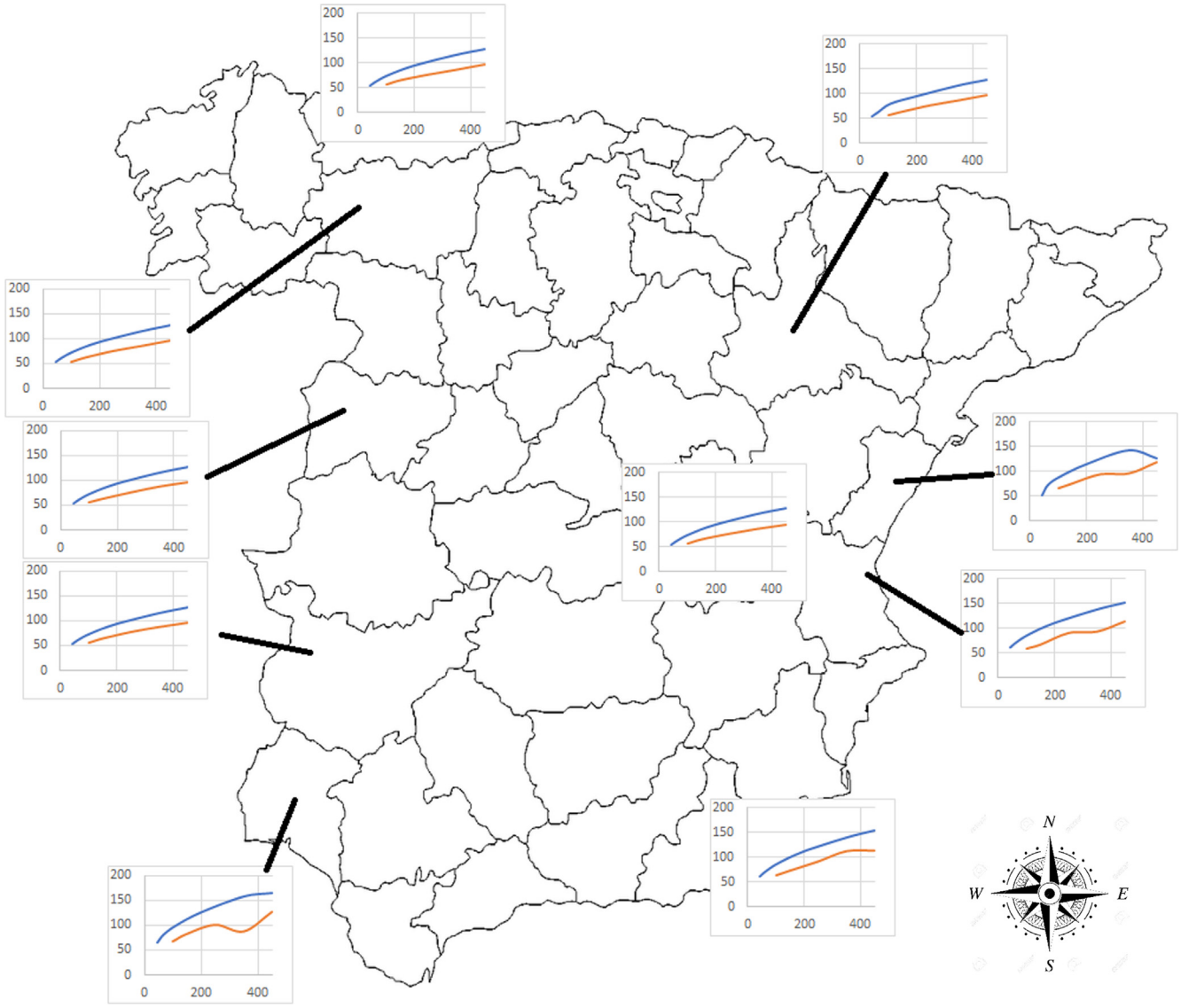

Fig. 5. Tower size (Height (m)) across the climatic regions por different production capacities (MW). Blue: Rankine; Red: Combined cycle.

cost. In the case of the regenerative Rankine cycle, Eq. (29) shows the correlation developed, while for the combined cycle, the correlation is presented in Eq. (30), where the temperature (T) is in Celsius (3.2–11.38 °C), the relative humidity (H = 0.64–0.82) is given as a fraction, the pressure (p = 0.89–1) is in atm and Power ranges from 40 to 450 MW.

$$\begin{aligned} T_{Height}(m) = (&-4.896\cdot10^{-5}\cdot T^2 - 5.027\cdot10^{-2}\cdot H^2 + 1.698\cdot10^{-3}\cdot p^2 \\ &- 7.840\cdot10^{-3}\cdot T\cdot H + 2.3175\cdot10^{-3}\cdot T\cdot p \\ &+ 0.467823\cdot H\cdot p + 4.6155\cdot10^{-3}\cdot T - 0.3066\cdot H - 0.3842\cdot p + 0.2837)\cdot \\ &Power^2 + (1.5485\cdot10^{-2}\cdot T^2 + \\ &+ 21.8527\cdot H^2 - 32.4850\cdot p^2 + 3.5460\cdot T\cdot H + 0.1973\cdot T\cdot p - 210.8925\cdot H\cdot p \\ &- 3.1559\cdot T + \\ &+ 139.613\cdot H + 223.761\cdot p - 148.1987)\cdot Power + (-1.9657T^2 \\ &- 1336.49058\cdot H^2 - 2991.472\cdot p^2 + \\ &- 178.296\cdot T\cdot H + 215.8447\cdot T\cdot p + 10534.978\cdot H\cdot p - 34.1144\cdot T \\ &- 6522.0254\cdot H - 4220.9457\cdot p + \\ &+ 4712.888) \end{aligned} \tag{29}$$

To validate the detailed model presented in Section 2 and Eq. (29), the two cooling towers of the *La Robla* power plant and the three ones corresponding to *Andorra* power plant are used. The two towers of the *La Robla* power plant serve two different groups of 284 MW and 370 MW each. The plant is located in the North-West of Spain, close to the city of León. The technical leaflet shows 100 m per tower [76]. Note that the height reported is the same but one of the groups has almost 25% larger production capacity. This correlation assigns 117 m and 128 m for the design condition of January. For the Andorra power plant, located in Teruel, the literature reports 107 m high and 81 m base diameter per group of 350 MW [77]. Eq. (29) overestimates again the height, 130 m, but the industrial tower matches the ratio between tower height and diameter given in Table 2. The overestimation may be due to the fact that in Eq. (19) the draft must be 10% larger than the pressure drop together with the fact that the packing of the towers is not reported and it can be different than the one used in the model.

$$T_{Height}(m) = (4.231\cdot10^{-5}\cdot T^2 + 0.223\cdot H^2 - 0.6739\cdot p^2 + 9.371\cdot10^{-3}\cdot T\cdot H + 4.962\cdot10^{-3}\cdot T\cdot p - 0.25301\cdot H\cdot p + - 1.2649\cdot10^{-2}\cdot T - 0.1701\cdot H + 1.4425\cdot p - 0.5751)\cdot Power^2 + (-1.1214\cdot10^{-2}\cdot T^2 - 131.094\cdot H^2 + 581.498\cdot p^2 + - 6.6526\cdot T\cdot H - 6.7797\cdot T\cdot p + 220.124\cdot H\cdot p + 11.7415\cdot T + 41.4477\cdot H - 1221.983\cdot p + 520.181)\cdot Power + (1.4349\cdot T^2 + 10677.289\cdot H^2 - 53566.636\cdot p^2 + 647.774876\cdot T\cdot H + 761.9941\cdot T\cdot p - 24850.89112755\cdot H\cdot p + - 1223.0867\cdot T + 2420.4049\cdot H + 114991.986\cdot p - 50867.282) \quad (30)$$

Eq. (30) is used to estimate the height of the tower of the *Elcogas* power plant. It is a combined cycle facility with a production capacity of 350 MW that had a natural draft cooling tower of 86 m of diameter and 122 m high [78]. For the design conditions of January at Puerto Llano, Ciudad Real (Spain), Eq. (30) predicts a tower size of 142 m. As in the case of the Rankine cycle, the correlation overestimates the size to make sure there is enough draft.

Similarly, correlations for the cost estimation of the cooling towers for the two different cycles are developed so that they can be used in conceptual design and/or implemented in current tools, i.e. [40,41,67,72]. The tower cost is estimated using Eq. (25) as presented in Section 2. For the regenerative Rankine the surrogate model is shown in Eq. (31), where the variable "Power" is given in kW and the rest of the variables are computed within the same ranges presented for Eqs. (29) and (30). Fig. 6 shows the fitting of the optimization results. The fitting is good, the correlation between the estimated and the computed values, R^2, is 0.9, but there are a few points with an error beyond 20%. Note that the cost estimated corresponds to the unit alone as given by [24].

$$Cost_{Tower}(€) = (655.3\cdot T^2 - 177564\cdot H^2 + 5926519\cdot p^2 - 5753\cdot T\cdot H - 104650\cdot T\cdot p - 288982\cdot H\cdot p + 95792\cdot T + 635954\cdot H - 10319667\cdot p + 4307004)\cdot Power + (10544\cdot T^2 + 20745600\cdot H^2 - 73074990\cdot p^2 + 2457264\cdot T\cdot H - 130129\cdot T\cdot p - 132420969\cdot H\cdot p - 1981510\cdot T + 74203328\cdot H + 243931768\cdot p - 137298587) \quad (31)$$

A similar analysis is carried out for combined cycle based power facilities. To capture the plant production capacity, Eq. (32) is developed, and Fig. 7 shows the fitting. In this case the fitting is better, with almost all values within 20%. The correlation between the estimated and the computed values, R^2, is 0.92.

$$Cost_{Tower}(€) = (0.5175\cdot T^2 + 2067\cdot H^2 - 7474\cdot p^2 + 114.5\cdot T\cdot H + 56.05\cdot T\cdot p - 4327\cdot H\cdot p - 150.1\cdot T + 62.05\cdot H + 17136\cdot p - 7602.8)\cdot Power^2 + (-344.6\cdot T^2 - 1009868\cdot H^2 + 2865079\cdot p^2 - 51263\cdot T\cdot H - 1084\cdot T\cdot p + 1930691\cdot H\cdot p + 46334\cdot T + 112221\cdot H - 6932563\cdot p + 3075848)\cdot Power + (30585\cdot T^2 + 77946022\cdot H^2 - 249464395\cdot p^2 + 4797070\cdot T\cdot H + 397748\cdot T\cdot p - 196626463\cdot H\cdot p - 4596664\cdot T + 29509822\cdot H + 624161048\cdot p - 290537291) \quad (32)$$

The cost of the construction of the unit includes the civil engineering, excavation, tunnels, electrics, etc. The value computed from Eqs. (31)–(32) only corresponds to the material as given by [24]. However, to compute the investment cost of the cooling tower, a ratio from the literature is used. It is reported that the direct cost of the project is around 10 times that of the tower itself [79,80]. Using this correction, for the average value of each capacity within the range 40–450 MW the cost is compared with the updated values from the ones estimated from Matche [41] and from the EPA [81]. In the supplementary material it is possible to see that while Matche [41] underestimates the costs, the correlation from the EPA consistently reports higher values. The average values for each capacity computed by the correlations are consistently in between. Note that neither of the estimations from the literature can cope with the effect of the weather conditions nor it is possible to know the exact weather conditions for which the towers estimated with the literature correlations are designed.

4.3. Water consumption in renewable based plants.

4.3.1. Water consumption across weather conditions

Apart from the structural design of the tower and its costing, water consumption is a major issue in the power industry [1–3,82–84]. Computing the consumption of water allows evaluating the water-energy nexus in the power industry as a function of the location of the facility as a first stage to evaluate the water footprint of any power system. The model described in Section 3 is used to determine the consumption of water for the two cycles, the regenerative Rankine and the combined cycle, for a set of weather conditions including air temperature, humidity and pressure.

To validate the models water consumption data from 18 towers from thermal power plants from the literature, 12 coal based gropus and 6 using natural gas, located in US [85], South Africa [9] Spain [86] and China [85,87] are compared with the ones predicted the model, see Table S1 in the supplementary material for the actual values. Using the average weather for each of the locations and Eqs. (33)–(34), the water consumption is estimated and compared with the ones reported. Note that the cycles of concentration (COC) must be corrected in some cases since the model in this work used 6. It is important to highlight that in some cases the COC value is not reported and the same value as in the model is assumed. Fig. 8 shows good agreement between the predicted and the reported ones in the case of combined cycle, while in the case of the Rankine cycle the values are underestimated unless drift is considered, blue symbols in the Figure. Note that while combined cycle facilites are newer, most coal based ones are older. More efficient cooling towers are explected for newer facilites. In addition, in the model description it was assumed that the drift was expected to be neglibible. Using a parameter estimation approach, the average drift of all the towers is 0.006 of the water flow fed to the column, see orange cycles in Fig. 8, with a R^2 of 0.85. It is a value lower than the one suggested by the rules of thumb [72], around 0.01, but still not negligible. Note that even thought it is not a good value, the results are

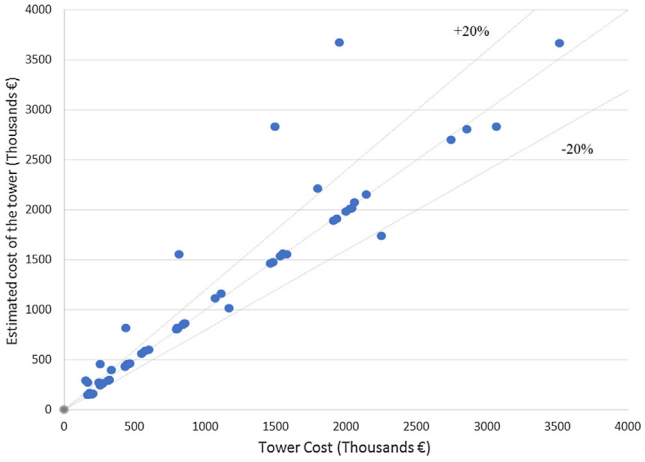

Fig. 6. Fitting of the effect of weather on cooling tower costs. Rankine cycle.

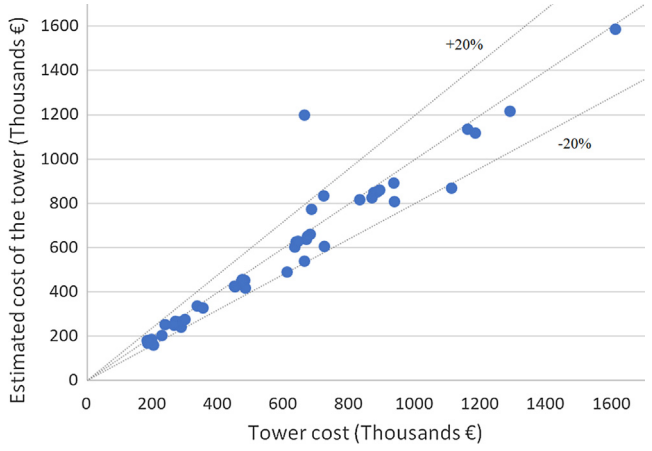

Fig. 7. Fitting of the effect of weather on cooling tower costs. Combined cycle.

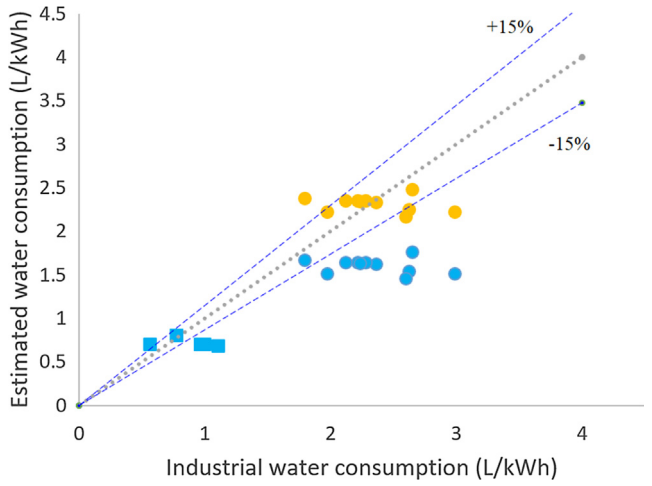

Fig. 8. Comparison between average water consumption and estimated one for different locations. Square: Combined cycle; Circle: Rankine. Blue: No drift; Orange: Drift.

within 15% error using generic settings for the cooling towers. Alternatively, the model can be used to simulate a particlar tower by using a parameter estimation approach as long as detailed data of its operation is provided including packing features and profiles of its operation.

Using the 10 locations and considering the weather of each month as an independent design condition, both cycles are studied for a fixed power production capacity of 350 MW. Drift is considered negligible. Fig. 9 presents the water consumption across different weather conditions in Spain. The integrated design of the combined cycle results in a reduction of water consumption almost by half with respect to the regenerative Rankine one, see Table 2. In terms of the effect of the weather conditions, the consumption of water increases to the South-East due to the humidity and temperature of the places. The higher the temperature, the larger the consumption of water. But humidity also plays a role. As a result, the water footprint of a power system where biomass thermal plants and CSP facilities have a high share is determined by the availability of the biomass, the solar incidence and the water to be consumed while operating the facility. Avoiding the Mediterranean coast will reduce water consumption, because of the high humidity coupled with high temperatures. Also at the North, characterized by high humidity, water consumption increases. Note, however, that water consumption must be relative to its availability, as exposed in the literature [60].

The results showed in Fig. 9 for the Rankine cycle range from 1 to 2 L/kWh, within the ones reported in the literature. In particular, while typical values from 1.8 L/kWh [82] to 2.6 L/kWh [8] are reported in the literature for coal thermal plants, values of 2.7 L/kWh and 3.2 L/kWh [82] are shown for nuclear and CSP plants respectively confirming the variability of the model results and the fact that CSP facilites are located in regions where they require larger consumption of water as well as the lower efficiency of the thermodynamic cycle. Furthermore, it can be seen that when a particular region is analyzed, see the state of Texas, the water consumption varies from location to location from 0.54 to 5.87 L/kWh [82] with an average value of 2.1 L/kWh [82]. With regards to the combined cycle, the consumption of water is around 0.8 L/kWh, see Fig. 9. In the literature values of 1 L/kWh are found for combined cycles [11,81]. In particular, for natural gas combined cycles values in the range of 0.7 L/kWh [82] to 1.4 L/kWh [8] are reported, for an average value of 1 L/kWh, while for integrated gasification combined cycle values of 1.3±0.4 L/kWh are shown in the literature [82]. For the state of Texas the average water consumption from combined cycle plants is 0.9 L/kWh [83]. In the literature the results for US consumption of water in the thermal production of electricity is 1.25 L/kWh on average, with a range from 0.7 for combined cycles to 2.0 for steam turbine when using cooling towers [84]. Thus, the results obtained in this work are within the ranges reported validating the model. Note that in the case of the combined cycle, only the stream from the steam turbine is condensed and both, the gas and the steam turbines, are responsible for the production of power.

4.3.2. Surrogate models for water consumption

The interactions between the variables prevent from a simple representation of the effect of the variables on the consumption of water. Using the set of results, surrogate models to estimate the water consumption as a function of the weather conditions of the site for both cycles are developed. As in the case of tower sizing, the aim is to provide easy to use models that can be useful in conceptual design, i.e. [40]. For the regenerative Rankine cycle, the surrogate model to compute the water consumption is given by Eq. (33), where the range of application is for the temperature, 3.2–32.4 °C, for the pressure, 0.89–1 atm, and for the humidity, 0.41–0.83. The good fitting can be seen in Fig. 10, with a correlation between the values estimated by the surrogate model and the computed ones by the detail one, R^2, is 0.94.

$$\begin{aligned} Water_{consumption}(L/kWh) = {} & -2.297\cdot10^{-4}\cdot T^2 + 0.798\cdot H^2 + 7.090\cdot p^2 \\ & + 2.200\cdot10^{-2}\cdot T\cdot H \\ & + 2.993\cdot10^{-2}\cdot T\cdot p - 0.515\cdot H\cdot p - 1.533\cdot10^{-2}T - 1.417\cdot H - 12.574\cdot p \\ & + 7.6256 \end{aligned} \tag{33}$$

Similarly, for the combined cycle, the correlation given by Eq. (34) is developed. The fitting is also good, as it can be seen in Fig. 11, with a correlation between the values estimated by the surrogate model and the computed ones by the detail one, R^2, of 0.92.

$$\begin{aligned} Water_{consumption}(L/kWh) = {} & -4.75\cdot10^{-4}T^2 + 1.255\cdot H^2 + 8.083\cdot p^2 \\ & + 3.453\cdot10^{-3}\cdot T\cdot H \\ & + 5.833\cdot10^{-2}\cdot T\cdot p + 1.292\cdot H\cdot p - 3.447\cdot10^{-2}T - 3.255\cdot H - 16.555p \\ & + 9.690 \end{aligned} \tag{34}$$

5. Conclusions

In this work a mathematical optimization framework is developed to conceptually compute the geometry of wet cooling towers and the water consumption rates for the sustainable design of the new power system where different energy sources and thermodynamic cycles are used. As a case study Spain has been used, a country very sensitive to water stress issues.

The optimal sustainable design of the tower results in the

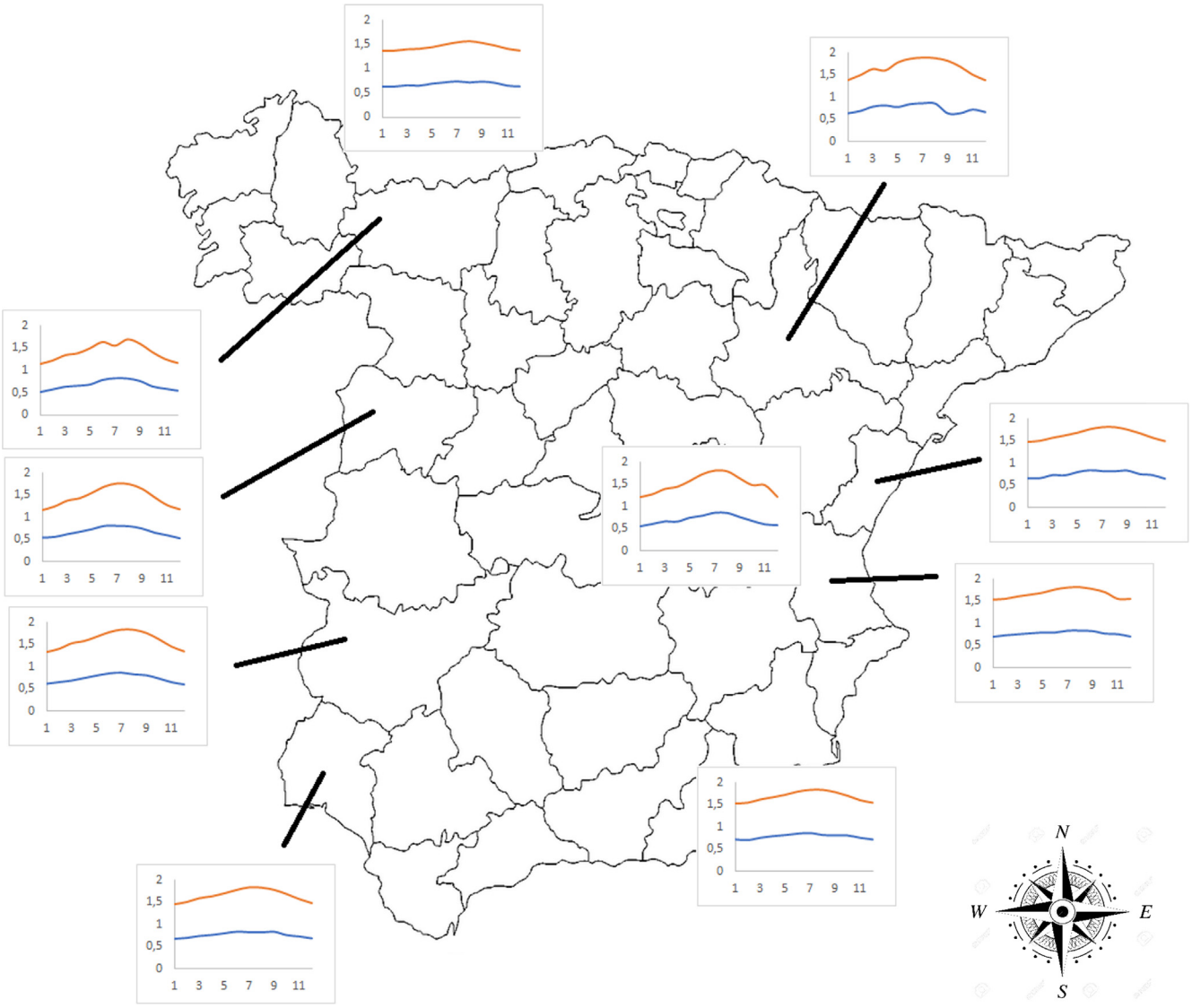

Fig. 9. Water consumption (L/kWh) across the climatic regions for 350 MW over the design conditions. Blue: Rankine; Red: Combined cycle. (For interpretation of the references to colour in this figure legend, the reader is referred to the web version of this article.)

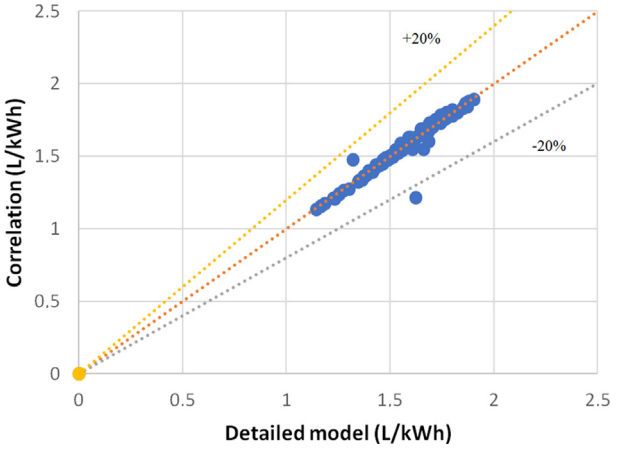

Fig. 10. Water consumption fitting. Rankine cycle.

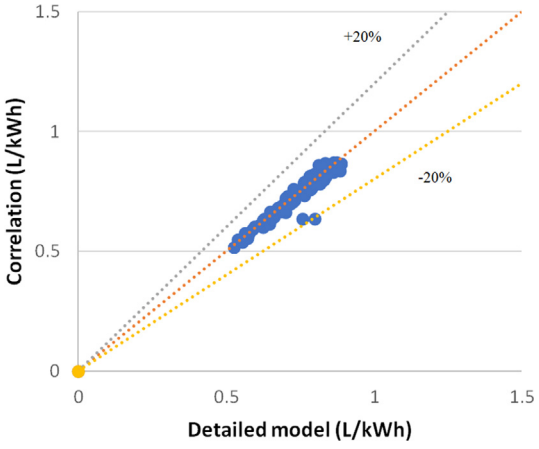

Fig. 11. Water consumption fitting. Combined cycle.

development of design guidelines in terms of geometric ratios that reduce material use and tower cost, maintaining tower performance and reducing water consumption. The geometry is validated versus actual towers; however, a higher lower section of the paraboloid is suggested from the analysis. Moreover, water consumption has been validated versus industrial data. Using the validated model, the operation of cooling towers across different climate areas is analyzed. It was shown that for the same production capacity, larger towers are to be installed to the South-East, where high temperatures and sometimes also moderate to high humidity are found. As a result of the weather conditions higher water footprint is reported also to the South-East. A large scale analysis comparing different cooling technologies would be needed to decide on the selection of the location of new facilities and their cooling system.

The analysis also allowed developing surrogate models to compute the water consumed, the tower size and its cost as a function of the humidity, the temperature and the atmospheric pressure for different power plant sizes. These correlations are useful to estimate the water stress of the energy transition from current fossil and nuclear based power to renewable one as well as to evaluate the water footprint of the next power production system where solar energy will play a key role.

CRediT authorship contribution statement

Lidia S. Guerras: Data curation, Investigation, Methodology, Validation, Software, Visualization, Writing - original draft. **Mariano Martín:** Conceptualization, Formal analysis, Funding acquisition, Investigation, Methodology, Project administration, Resources, Supervision, Visualization, Writing - original draft, Writing - review & editing.

Declaration of Competing Interest

The authors declare that they have no known competing financial interests or personal relationships that could have appeared to influence the work reported in this paper.

Acknowledgments

The authors would like to acknowledge JCYL Grant number SA026G18 and the staff at La Robla Power plant.

Appendix A. Supplementary material

Supplementary data to this article can be found online at https://doi.org/10.1016/j.apenergy.2020.114620.

References

[1] Tosolas SD, Karim MN. Faruque Hasan, MM Optimization of water energy nexus: a network representation-based graphical approach. Appl Energy 2018;224:230–50.
[2] Gjorgiev B, Sansavini G. Electrical power generation under policy constrained water-energy nexus. Appl Energy 2018;201:568–79.
[3] Nouri N, Balali F, Nasiri A, Seifoddini H, Otieno W. Water withdrawal and consumption reduction for electrical energy generation systems. Appl Energy 2019;248:196–206.
[4] Dehaghani ST, Ahmadikia H. Retrofit of a wet cooling tower in order to reduce water and fan power consumption using a wet/dry approach. Appl Therm Eng 2017;125:1002–14.
[5] Luceño JA, Martín M. Two-step optimization procedure for the conceptual design of A-frame systems for solar power plants. Energy 2018;165:483–500.
[6] Harte R, Kratzin WB. Large scale cooling towers as part of an efficient and cleaner energy generating technology. Thin Walled Struct 2002;40:651–64.
[7] Zhai H, Rubin ES. Performance and cost of wet and dry cooling systems for pulverized coal power plants with and without carbon capture and storage. Energy Policy 2010;38:5653–60.
[8] Macknick J, Newmark R, Heath G, Hallett KC, A Review of Operational Consumption and Withdrawal Factors for Electricity Generating Technologies; National Renewable Energy Laboratory Technical Report; NREL/TP-6A20-50900; National Renewable Energy Laboratory: Golden, CO, USA; 2011.
[9] A simple model to help understand water use at power plants. Energy Initiative 2012 https://sequestration.mit.edu/pdf/2012_AD_HJH_WorkingPaper-WaterUse_at_PowerPlants.pdf.
[10] Torcellini P, Long N, Judkoff R, National Renewable Energy Laboratory (NREL). Consumptive Water Use for US Power Production; 2003.
[11] Maulbetsch JS, DiFilippo MN. California Energy Commission, PIER Energy-Related Environmental Research. Cost and Value of Water Use at Combined-Cycle Power Plants; 2006. CEC-500-2006-034.
[12] Ali B, Kumar A. Development of water demand coefficients for power generation from renewable energy technologies. Energ Convers Manage 2017;143:470–81.
[13] Wan L, Wang C, Wenjia C. Impacts on water consumption of power section in major emitting economies under INDC and longer terms mitigation scenarios: An input – output based hybrid approach. Appl Energy 2019;184:26–39.
[14] Peer RAM, Sanders KT. The water consequences of a transitioning US power sector. Appl Energy 2018;210:613–22.
[15] Kroger DG. Air-cooled heat exchangers and cooling towers: thermal-flow performance evaluation and design, vol. II. Tulsa: Pennwell: Oklahoma; 2004.
[16] Tanimizu K, Hooman K. Natural draft dry cooling tower modelling. Heat Mass Transf 2013;49:155–61.
[17] Busch D, Harte R, Kratzig W, Montag U. New natural draft cooling tower of 200 m of height. Eng Struct 2002;24:12.
[18] Li X, Duniam S, Gurgenci H, Guan Z, Veeraragavan A. Full scale experimental study of a small natural draft dry cooling tower for concentration solar thermal power plant. Appl Energy 2017;193:15–27.
[19] Dupreez AF, Kroger DG. Effect of wind on performance of a dry-cooling tower. Heat Recov Syst CHP 1993;13(2):139–46.
[20] Zhang G, He S, Zhang Z, Xu Y. Wang R Economic analyses of Natural draft dry cooling towers precooled using wetted media. Proc Engng 2017;205:423–30.
[21] Gould PL, Kratzig WB. Cooling tower structures. In Structural Engineering Handbook. Wai-Fah C. Ed CRC Press Boca Raton; 1999.
[22] Busch D, Harte R, Krätzig WB, Montag U. New natural draft cooling tower of 200 m of height. Eng Struct 2002;24(12):1509–21.
[23] Lang C, Strauß J. Natural Draft Cooling Tower Design and Construction in Germany - Past (since 1965), Present and Future. 2011, http://www.ibb-lang.de/mediapool/135/1355294/data/Publikationen/Lang_SEWC2011.pdf [accessed January 2019].
[24] Buys JD, Króger DG. Cost Optimal design of dry cooling towers through mathematical programming techniques. Trans ASME 1989;111:322–7.
[25] Kloppers JC, Kröger DG. Cost optimization of cooling tower geometry. Eng Opt 2004;36(5):575–84.
[26] Lemouari M, Boumaza M, Kaabi A. Experimental analysis of heat and mass transfer phenomena in a direct contact evaporative cooling tower Energy Convers. Manag 2009;50:1610–7.
[27] Kloppers JC, Kröger DG. A critical investigation into the heat and mass transfer analysis of counterflow wet cooling towers. Int. J. Heat Mass Transf 2005; 48; 765–77.
[28] EPA (Environmental Protection Agency). A method for predicting the performance of natural draft cooling towers Pacific Northwestern Water Laboratory; 1970.
[29] Williamson N, Behnia M, Armfield SW. Thermal optimization of a natural draft wet cooling tower. Int J Energy Res 2008;32(14):1349–61.
[30] Kreith F, Goswami DY. The CRC handbook of mechanical engineering. 2nd Edition CRC Press Boca Ratón; 2005.
[31] Xu C, Wang Z, Li X, Sun F. Energy and exergy analysis of solar power tower plants. Appl Therm Eng 2011;31(17–18):3904–13.
[32] Qi X, Liu Z, Li D. Performance characteristics of a shower cooling tower. Energy Convers Manage 2007;48:193–203.
[33] Ifaei P, Rashidi J, Yoo C. Thermoeconomic and environmental analyses of a low water consumption combined steam power plant and refrigeration chillers – Part 1: Energy and economic modelling and analysis. Energy Convers Manage 2006;123:610–24.
[34] Ifaei P, Rashidi J, Yoo C. Thermoeconomic and environmental analyses of a low water consumption combined steam power plant and refrigeration chillers-Part 2: Thermoeconomic and environmental analysis. Energy Convers Manage 2006;123:625–42.
[35] Sun Y, Guan Z, Gurgenci H, Wang J, Dong P, Hooman K. Spray cooling system design and optimization for cooling performance enhancement of natural draft dry cooling tower in concentrated solar power plants. Energy 2019;168:273–84.
[36] Queiroz JA, Rodrigues VMS, Matos HA, Martins FG. Modelling of existing cooling towers in ASPEN PLUS using an equilibrium stage method. Energy Convers Manage 2012;64:473–81.
[37] Martín L, Martín M. Optimal year-round operation of a Concentrated Solar Energy Plant in the South of Europe. Appl Therm Eng 2013;59:627–33.
[38] Serna-González M, Ponce-Ortega JM, Jiménez-Gutiérrez A. MINLP optimization of mechanical draft counter flow wet-cooling towers. Chem Eng Res Des 2009;88(5–6):614–25.
[39] Gao M, Zhang L, Wang NN, Shi YT, Sun FZ. Influence of non-uniform layout fillings on thermal performance for wet cooling tower. Appl Therm Eng 2016;93:549–55.
[40] Sinnott R, Towler G. Chemical Engineering Design. Principles, practice and economics of plant and process design. 2ª ed. Elsevier Butterworth-Heinemann, Oxford.
[41] Matche www.marche.com [accessed March 2019].
[42] Martín M, Martín M. Cooling limitations in power plants: optimal multiperiod design of natural draft cooling towers. Energy 2017;135:625–36.
[43] Jagadeesh T, Reddy KS. Performance analysis of the natural draft cooling tower in different season. IOSR J Mech Civil Eng 2013;7(5):19–23.
[44] Ludovisi D, Garza IA. Water consumption of cooling towers in different climatic zones of U.S. Proceedings of the ASME 2015 power and energy conversion conference. 2015.
[45] Ayoub A, Gjorgiev B, Sansavini G. Cooling towers performance in a changing

climate: Technoeconomic modelling and design optimization. Energy 2018;160:1133–43.
[46] Krahé D, Beisheim B, Engell S. Decision support for energy-efficient cooling tower operation using weather forecasts. Chem Eng Trans 2016;52:1009–14.
[47] Smrekar I, Kustrin I, Omarn J. Methodology for evaluation of cooling tower performance – Part 1: description of the methodology. Energy Convers Manage 2011;52:3257–64.
[48] Peck JJ, Smith AD. Quantification and regional comparison of water use for power generation: A California ISO case study. Energy Rep 2017;3:22–8.
[49] Byers EA, Hall JW, Amezaga JM. Electricity generation and cooling water use: UK pathways to 2050. Global Environ Change 2014;25:16–30.
[50] Gao M. Sun FZH Experimental study regarding the evolution of temperature profiles inside wet cooling tower under crosswind conditions Int. J Therm Sci 2014;86:284–91.
[51] Li X, Gurgenci H, Guan Z, Wang X, Xia L. A review of the crosswind effect on the natural draft cooling towers. Appl Therm Eng 2019;150:250–70.
[52] Khamis Mansour M, Hassab MA. Innovative correlation for calculating thermal performance of counterflow wet-cooling tower. Energy 2014;74:855–62.
[53] ASHRAE (Archives American Society of Heating). Equipment Guide, Chapter 3, American Society of Heating, Refrigerating, and Air-Conditioning Engineers, Inc., Atlanta, Ga., USA; 1983.
[54] Qureshi BA, Zubair SM. Prediction of evaporation losses in wet cooling towers. Heat Transfer Eng 2006;27(9):86–92.
[55] Vengateson U. Cooling towers: estimate evaporation loss and makeup water requirements. CEP April; 2017.
[56] Zhang H, Feng X, Wang Y. Comparison and evaluation of air cooling and water cooling in resource consumption and economic performance. Energy 2018;154:157–67.
[57] IEA (International Energy Agency). Water for energy: Is energy becoming a thirstier resource? 2012 https://www.iea.org/media/publications/weo/WEO_2012_Water_Excerpt.pdf [accessed December 2018].
[58] Electrical Network of Spain. www.ree.es [accessed July 2018].
[59] Adapated to IGN (National Geographic Institute). https://www.ign.es/espmap/mapas_clima_bach/pdf/Clima_Mapa_01_texto.pdf [accessed January 2019].
[60] Martín M. RePSIM metric for design of sustainable renewable based fuel and power production processes. Energy 2016;114:833–45.
[61] Oliver JGJ, Bouwman AF, Berdowski JJM, Veldt C, Bloos JPJ, Visschedijk AJH, et al. Sectoral emission inventories of greenhouse gases for 1990 on a per country basis as well as on 1°×1°. Environ Sci Policy 1999;2(3):241–63.
[62] Katimber. http://www.kaltimber.com/blog/2017/6/19/how-much-co2-is-stored-in-1-kg-of-wood/ [accessed January 2019].
[63] Vidal M, Martín M. Optimal coupling of biomass and solar energy for the production of electricity and chemicals. Comp Chem Eng 2015;72:273–83.
[64] Ghobeity A, Noone CJ, Papanicolas CN, Mitsos A. Optimal time-invariant operation of a power a water cogeneration solar-thermal plant. Sol Energy 2011;85(9):2295–320.
[65] Morin G, Richter P, Nitz P. New method and software for multi-variable techno-economic design optimization of CSF plants. www.mathcces.rwth-aachen.de/_media/5people/richter/pascalrichter-2010-solarpaces.pdf [accessed December 2012].
[66] Palenzuela P, Zaragoza G, Alarcón-Padilla DC, Guillén E, Ibarra M, Blanco J. Assessment of different configurations for combined parabolic-trough (PT) solar power and desalination plants in arid regions. Energy 2011;36(8):4950–8.
[67] Wallas SM. Chemical process equipment. Newton MA: Selection and Design. Butherworth Heinemann; 1990.
[68] León E, Martín M. Optimal production of power in a combined cycle from manure based biogas. Energy Convers Manage 2016;114:89–99.
[69] Moran MJ, Shapiro HN. Fundamentals of engineering thermodynamics. 1th ed. New York: Wiley & Sons; 2003.
[70] Cheremisinoff NP, Chremisinoff PN. Cooling Towers: Selection, design and practice. Ann Arbor, Michigan, Ann Arbor Science Publishers, 347; 1981.
[71] Geankoplis CJ. Transport processes and unit operations. 3rd ed. Prentice Hall Upper Saddle River: New Jersey. U.S.A; 1993.
[72] Perry RH, Green DW. Perry's Chemical Engineer's Handbook McGraw-Hill: New York. U.S.A; 1997.
[73] Coulson J, Richardson J. Chemical engineering. UK: Butterworth Heinemann; 1999.
[74] Almási J. Approximate determination of cooling tower dimensions. Period Polytech Civil Eng 1981;25(1–2):95–110.
[75] Fatigati M. Conserving Water in Ethanol Plants. Western Region BBI Biofuels Workshop 2006. San Diego CA. http://www.bbibiofuels.com/biofuelsworkshop/2006/docs/speakerpapers/west/bww/BWW06-14-Fatigati.pdf [accessed November 2018].
[76] Union Fenosa. Central Térmica La robla http://www.unionfenosa.es/webuf/wcm/connect/430b6200495cc71ebd17fd8205e0cb4d/folleto_tecnico_central_termica_de_la_robla.pdf Last accessed August 2019.
[77] https://es.wikipedia.org/wiki/Central_t%C3%A9rmica_de_Andorra. Last accessed August 2019.
[78] Europapress 2018 La torre de refrigeración de Elcogas, demolida tras detonar 466 microcargas de dinamita. In Spanish. https://www.europapress.es/castilla-lamancha/noticia-torre-refrigeracion-elcogas-demolida-detonacion-466-microcargas-dinamita-20180628162541.html. Last accessed August 2019.
[79] McDowell B. Comprehensive Technical Feasibility and Cost Evaluation Study. Alcoa Warrick Power Plant Project No. 85014; 2018.
[80] US Nuclear regulatory commission. Office of Nuclear reactor regulation. Dradt Enviromental statement for selection of the preferred closed cycle cooling system at INDIAN point unit no 2; 1976.
[81] EPA. Detailed Information on Technologies/Development of Unit Costs §316(b) EEA Appendix A for New Facilities; 2000.
[82] Stillwell AS, King CW, Webber ME, Duncan IJ, Hardberger A. The energy-water nexus in Texas. Ecol Soc 2011; 16 (1): 2 http://www.ecologyandsociety.org/vol16/iss1/art2/.
[83] Scanlon BR, Reedy RC, Duncan I, Mullican WF, Young M. Controls on water use for thermoelectric generation: case study Texas, U.S. Environ Sci Technol 2013;47:11326–34. https://doi.org/10.1021/es4029183.
[84] Lee U, Han J, Elgowainy A. Wang M Regional water consumption for hydro and thermal electricity generation in the United States. Appl Energy 2018;201:661–72.
[85] Xia L, Li J, Ma W, Gurgenci H, Guan Z, Wang P. Water consumption comparison between a natural draft wet cooling tower and a natural draft hybrid cooling tower—an annual simulation for Luoyang conditions. Heat Trans Eng 2017;38(11–12):1034–43.
[86] Sesma-Martí D. The River's Light: Water Needs for Thermoelectric Power Generation in the Ebro River Basin. 1969–2015. Water 2019; 11: 441.
[87] Jiang Daqian, Ramaswami Anuradha. The 'thirsty' water-electricity nexus: field data on the scale and seasonality of thermoelectric power generation's water intensity in China. Environ Res Lett 2015;10(2):024015. https://doi.org/10.1088/1748-9326/10/2/024015.